energies

Review

The Controls of Laminae on Lacustrine Shale Oil Content in China: A Review from Generation, Retention, and Storage

Qiyang Gou [1] and Shang Xu [2,*]

[1] Key Laboratory of Tectonics and Petroleum Resources, Ministry of Education, China University of Geosciences, Wuhan 430074, China
[2] School of Geosciences, China University of Petroleum, Qingdao 266580, China
* Correspondence: xushang0222@163.com

Abstract: The successful development of shale oil in China has claimed that laminated shale is a favorable lithofacies for the effective extraction of petroleum. Clarifying the role of laminae in shale oil generation, migration, storage, and enrichment is urgent and important. Starting from the describing and classifying of the lamina, the common methods and terms used to delineate lamina types are briefly summarized. The results of different schemes are often mutually inclusive, which prompted scholars to work towards a unified division scheme. The influencing factors of oil retention in shale systems, including organic matter (OM) type, total organic carbon (TOC) content, OM maturity, mineral composition, pore structure, and preservation conditions, are systematically discussed. Subsequently, comparative work on source rock quality, reservoir properties, and hydrocarbon expulsion efficiency of shales with different laminar structures is carried out. The comparison results of shale with different rock structures reveal that the laminated shale has a high expulsion efficiency. However, the strong oil generation capacity and superior storage space of laminated shale synergistically control the considerable amount of retained oil in the shale system. Especially the oil mobility of laminated shale is also considered because of great pore size and pore connectivity. The fine evaluation of laminar structure and prediction of laminar distribution has great significance for the selection of shale oil "sweet spot area" or "sweet spot interval".

Keywords: shale oil; lamina structure; oil-bearing; influencing factors; enrichment mechanism

Citation: Gou, Q.; Xu, S. The Controls of Laminae on Lacustrine Shale Oil Content in China: A Review from Generation, Retention, and Storage. *Energies* **2023**, *16*, 1987. https://doi.org/10.3390/en16041987

Academic Editor: Nikolaos Koukouzas

Received: 1 February 2023
Revised: 10 February 2023
Accepted: 15 February 2023
Published: 16 February 2023

1. Introduction

In recent years, shale oil, with enormous resource potential, has gradually become an increasingly important component of the global hydrocarbon endowment [1–4]. With the application of horizontal drilling and multi-stage hydraulic fracturing technologies, the large-scale development of shale oil in the United States has been obtained [1]. From 2009 to 2019, the annual production of oil molecules from the shale formations, e.g., Wolfcamp Formation in the Permian Basin, Bakken Formation in the Williston Basin, and Eagle Ford Formation in the Maverick Basin, has increased to 2.83 billion barrels [5]. This has changed the energy landscape of the U.S.A., driving it to become a net exporter of energy [6,7]. Similarly, results of drilling in several petroliferous strata, e.g., Qingshankou Formation of the Songliao Basin [2,8], Kongdian Formation and Shahejie Formation of the Bohai Bay Basin [9–11], Xin'gouzui Formation and Qianjiang Formation of the Jianghan Basin [12,13], Yanchang Formation of the Ordos Basin [14–16], Lucaogou Formation and Fengcheng Formation of the Junggar Basin [3,17], has documented the substantial hydrocarbon liquids resource in China. Estimates have suggested that the proven geological reserves of China exceed 13×10^8 t [14,18]. An annual shale oil production exceeded 270×10^4 t in 2021, which makes it possible for shale oil to become a new energy supply [3,18,19].

As for North America, commercial shale oil formations are generally located in marine sedimentary environments [1,20,21]. In contrast, the shale oil reserves in China are mainly

derived from lacustrine shale [2,22,23]. The main difference between marine and lacustrine shale systems is their sensitivity to climate change and the associated changes in sea level or lake level [1]. Generally, frequent lake level changes associated with climate in the lake basin have led to the development of a large number of different types of lamina in lacustrine shale systems [1,22,24–26]. The heterogeneity of the lacustrine shale system becomes more prominent. However, the expansion of exploration indicates that the breakthrough in continental shale mainly comes from shale series with well-developed laminae [22,27,28]. More importantly, statistics of producing wells suggest about 70% of oil flows produce from laminated shale lithofacies [29,30]. In other words, the extraction of petroleum for lacustrine shale systems in China has shown that laminated shales are favorable lithologies, which is also supported by the presence of residual asphaltene along pavement planes and between laminae fractures in core observations [9–11]. Therefore, systematically evaluating the influence of lamina structure on shale oil enrichment is the basis for answering the question of high production from oil wells and is also the key to achieving efficient shale oil development.

To date, the works of pioneers have realized that laminar structure is closely related to organic matter enrichment, reservoir space, and oil and gas production [9–11,15]. However, the diversity in different laminae and how they affect the accumulation of shale oil have not yet been satisfactorily investigated. In order to fully understand the role of laminae in the process of shale oil enrichment, a systematic review work on the influence of laminae on shale oil generation, migration, retention, and storage is carried out. In this work, we first summarized the most common division schemes and terms in the literature relating to laminae in the shale system. Subsequently, the influencing factors, including OM type, TOC content, OM maturity, mineral composition, pore structure, and preservation conditions, of shale oil content are presented. In such cases, the effects of laminae on shale oil enrichment are systematically discussed in terms of controlling the generation, discharge, retention, and storage of hydrocarbons in shale systems. This work is anticipated to offer a theoretical foundation for shale oil resource assessment and promising exploration area prediction.

2. Classification and Terminology for Shale Laminae

A lamina is the smallest megascopic layer without internal layers in a sedimentary succession [31,32]. Laminae commonly form in a relatively short period of time, typically within a year or more [31,33]. Within a relatively small vertical scale, the thickness of lamina usually ranges from μm to mm [34–36]. Among the multitude of division schemes, the mineral composition is the parameter most often involved in describing and classifying lamina in shale systems [15,34,37–39]. In such cases, organic matter laminae, calcite laminae, dolomite laminae, clay laminae, and quartz-feldspar laminae are identified as five major types of laminae [11,15,40–43] (Figure 1A–C). It is worth noting that the types of laminae are also distinctly different in various basins or regions. For example, calcite laminae are well-developed in the Dongying Sag [35,44,45], while dolomite laminae and felsic laminae are more prominent in the Cangdong Sag [27,46]. In addition, the clay laminae and organic matter laminae are widely observed in the Triassic Yanchang Formation of the Ordos Basin [15]. Especially some special laminae, e.g., tuffaceous laminae, are also widely observed in the lacustrine sedimentary basin (Figure 1C) [15,47].

The thickness is another essential attribute to describing laminar type [35,48–50]. Following the usage of Ingram [48], laminae thickness is smaller than 10 mm, which was subsequently divided into thick laminae (thickness between 3 and 10 mm) and thin laminae (thickness < 3 mm). Different people in the geological literature also seem to use other terms to describe laminated thickness. One of the categories is layer (100–500 mm), thin lamina (10–100 mm), lamina (1–10 mm), and sheet (<1 mm) [49]. The demarcation line between the lamina and layer, according to the work of Liu et al. [35], is placed at 1 mm (lamina < 1 mm and layer > 1 mm). Additionally, Zeng et al. [40] further pointed out that laminae with a thickness range of 0.2–1 mm can be defined as wide laminae, while those with a thickness of less than 0.2 mm are named fine laminae (Figure 1D–F).

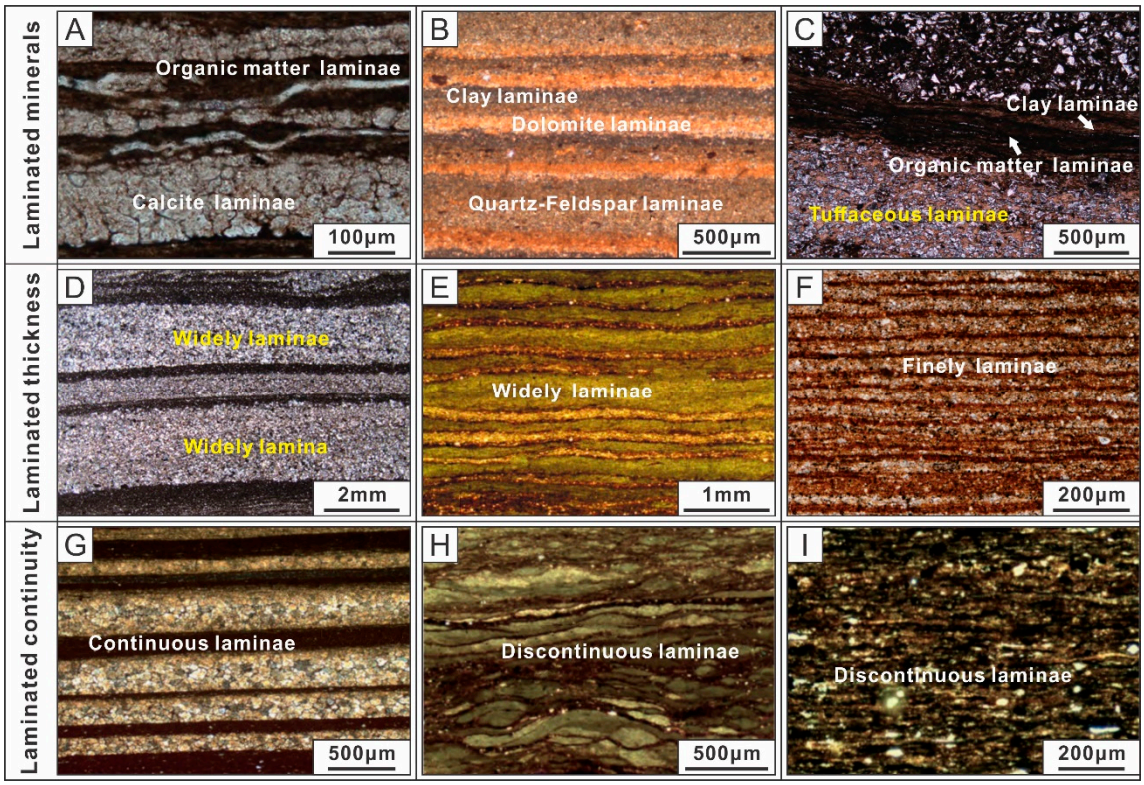

Figure 1. Terminology for the description of laminae, mainly including mineral composition, thickness, and continuity, in different classification schemes. (**A**–**C**) The types of laminae described by the mineral composition of laminae. (**D**–**F**) The types of laminae described by the thickness of laminae. (**G**–**I**) The types of laminae described by the continuity of laminae. Modified after [11,15,40–43].

Lamina can be continuous and discontinuous within a small lateral extent. Thus, the terms continuous laminae and discontinuous laminae are also used to capture laminar structure [33,40]. The practical examples of this type have been presented by thin section images (Figure 1G–I). In addition, some scholars proposed a combination of continuity, shape, and geometry to delineate the lamina. As a result, a total of 12 different types of lamina are identified, and a detailed description can be found in Lazar et al. [33].

Other methods for dividing shale lamination, including lamination color (can divide into dark laminae and bright laminae) and grain size, are also partially mentioned [50,51]. We also note that the results of the different division schemes are often mutually inclusive. For example, the wide laminae shown in Figure 1D belongs to both felsic laminae and continuous, parallel laminae. As a result of the multivariate division scheme, the comparability of research results of different scholars is reduced. Therefore, it is worth exploring how to establish a unified laminar division scheme that can take into account various geological attributes.

3. Controlling Factors of Oiliness in Shales

3.1. Restriction of Organic Matter Properties on Oiliness

The breakage of chemical bonds in organic matter is the fundamental process of oil generation [23,52,53]. The weak bonds, such as the aromatic ether bonds (-O) and thioether bonds (-S), will break with an increase in thermal maturity [54]. Under intense heat, the organic matter decomposes partly into the asphalt and partly into the oil. Moreover, asphalt could be further converted to petroleum with increasing temperature [55,56]. Accordingly, maturity and oil content showed a trend of synergistic increase in the early stage [9,57–59] (Figure 2). However, excessive maturity can also lead to a decrease in the oil generation capacity of kerogen. The oil generated in the early stage will be reduced by

secondary cracking [60]. At the same time, the increase in hydrocarbon content will create overpressure and generate associated fractures, which will improve the migration capacity of hydrocarbons and thus further reduce the oil content of shale reservoirs [58,61]. Shale oil exploration practices suggested that the Ro (i.e., vitrinite reflectance) of oil generally plays between 0.5% and 1.6% [58,62]. In particular, the work of Yang and Zou [63] claimed that the amount of retained oil in shale systems Ro of 0.9–1.3% is superior.

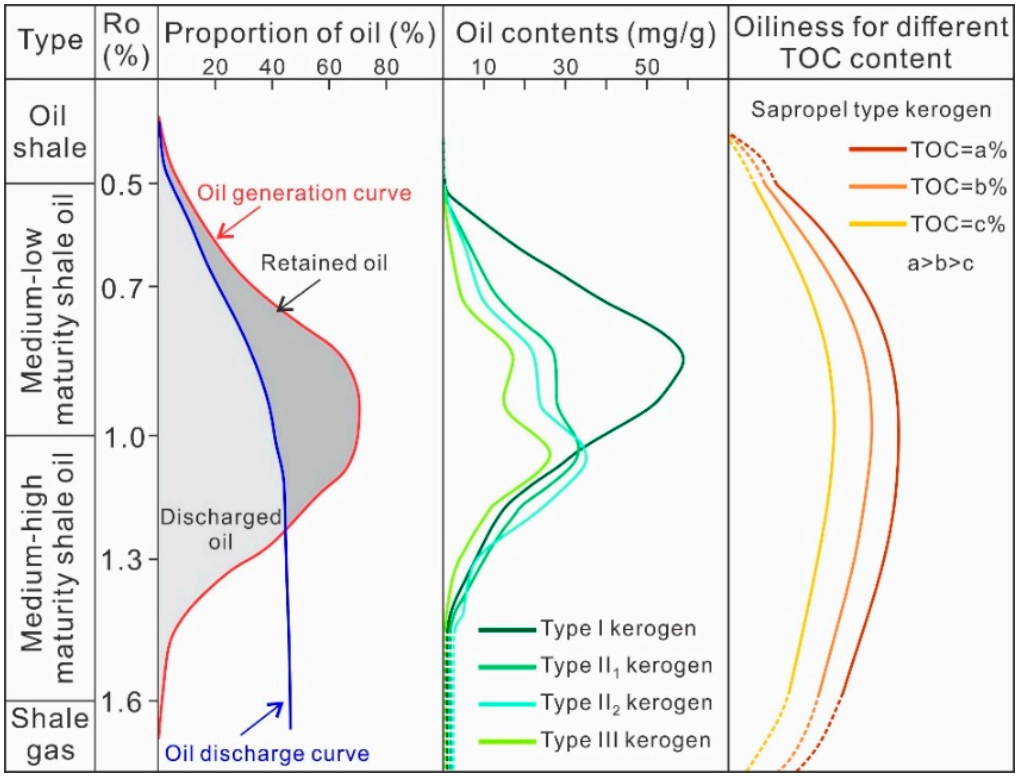

Figure 2. Oil-bearing characteristics of shales with different organic matter type, content, and maturity. Modified after [9,57–59].

Kerogen, an organic macromolecule comprising semi-random crosslinked nuclear structures, is the origin of petroleum [52]. The classification of kerogens from sedimentary source rocks into three main types, i.e., type I, type II, and type III [64]. The type I kerogen is highly aliphatic, with an H/C atomic ratio, frequently > 1.5, and the oxygen content is often low. The H/C and O/C atomic ratios of immature type II kerogen are ~1.3 and ~0.15, respectively. Meanwhile, type III kerogen is frequently derived from higher plant debris, with an H/C atomic ratio of less than 0.8 [65]. Great efforts have shown that Type I or II kerogen, with a highly effective organic carbon ratio, possess great oil generation capacity [64–67]. The thermal simulation experiment conducted by Zhao et al. [59] pointed out that when Ro was 0.6–1.0%, the hydrocarbon content per unit organic matter for type I kerogen is more than one times higher than that of other types of kerogen (Figure 2). The work of Sun et al. [68] also noted a positive correlation between the hydrogen index and retained content. However, some geological observation suggests that type II kerogen could possess more shale oil deposits than type I kerogen [69]. They attribute this phenomenon to the high hydrocarbon expulsion efficiency of shales with type I kerogen and relatively limited storage space [57,69].

Organic matter abundance also has a significant impact on shale oil content (Figure 2). Typically, a high total organic carbon (TOC) content means more oil can be generated, thus contributing to an increase in the hydrocarbon content of the reservoir [26,58,70]. Additionally, previous works have shown that an increase in TOC also increases organic acids content during the hydrocarbon generation process, which promotes the development of disso-

lution pores and recrystallized interparticle pores related to carbonate minerals [71–74]. On this premise, the enrichment degree of shale oil has also improved [29,75,76]. Notwithstanding, the oiliness does not always monotonously increase with an increase in TOC. For example, Zhao et al. [77] pointed out that the effect of TOC on shale oil content is not significant when the TOC of shale in the Kongdian formation exceeds 4%. Other inflection points, such as TOC at 1.8% [78], 2% [59,79,80], and 2.6% [78], have also been reported in different regions. In addition, Hu et al. [26] noted that the storage of hydrocarbons is unfavorable after TOC greater than 10% in the salinized lake basin.

3.2. Restriction of Mineral Composition on Oiliness

One of the mechanisms of mineral composition affecting shale oil is the adsorption of petroleum on the mineral surface [81,82]. In other words, the retention amount of shale oil on mineral surfaces is attributed to specific surface areas [83,84]. In other words, varied mineral types have different specific surface areas, which could influence the amount of adsorbed oil. Based on hydrocarbon-solution adsorption studies, the adsorption capacity of feldspar for asphaltene is about 7 mg/g, while that of quartz is 4.5 mg/g [85]. Mohammadi and Sedighi [86] also reported that the maximum adsorption capacity of calcite is relatively low, with a value of 2.16 mg/g. Similarly, Li et al. [83] obtained the amount of oil adsorbed by quartz and carbonate minerals as 3 mg/g and 1.8 mg/g, respectively. Furthermore, their work has supplemented the oil adsorption capacity of clay minerals, which can reach 18 mg/g [83]. However, some studies have reported that only 5–10% of oil molecules are adsorbed on the surfaces of mineral particles [59]. It is reasonable to speculate that the retention effect of minerals adsorption on shale oil is negligible compared to that of organic matter (~179 mg/g) [87]. Notwithstanding, the mechanism by which mineral particles control oil content by influencing the pore structure cannot be ignored [88,89]. For example, Feng et al. [90] noticed that the increase of quartz and clay content in the Qingshankou Formation shales improves the reservoir space, which in turn promotes the enrichment of shale oil. In addition, Cheng et al. [91] presented that the carbonate content of the Shahejie Formation shale exhibited negative relationships with shale porosity, which leads to a significant reduction of retained oil contents.

3.3. Restriction of Pore Structure on Oiliness

Adsorbed oil and free oil are two primary forms of petroleum in a shale system [54,92]. The enrichment of oil molecules in shale reservoir experiences the process of adsorption on the surface of organic matter, mineral particles, and pores, as well as freeing in pores and fractures core [93,94]. Molecular dynamics simulation conducted by Wang et al. [95] revealed that multiple adsorbed layers of liquid hydrocarbons are stored in nanopores. The thickness of each adsorbed oil film is counted as about 0.48 nm [95,96]. Based on the hydrocarbon vapor adsorption and pore calculation model, similarly, Dang et al. [94] noticed that within the micropore and mesopore range, the average thickness of the adsorbed oil film increases between 0.19 nm and 1.59 nm, and the number of adsorption layers increases from one to three. On the other hand, the average thickness of the adsorbed oil film increases significantly between 1.59 and 1.81 nm for the macropore region, and the number of adsorption layers increases from three to four or five. Chen et al. [97] argued that 80% of shale oil is distributed in macropores. The occurrence states and content of shale oil in pores with different scales are distinct.

Based on the data of typical shale oil systems in China, we performed a comparative analysis of the relationship between the porosity and oil content of shale [46,79,98–100] (Figure 3). We note that although the influence degree of porosity on S_1 or oil saturation varies in different regions, the overall performance is that the oil content increases with the increase of porosity (Figure 3). Additionally, the positive correlation between pore volume and oil content has also been widely reported [70,87,89]. Moreover, Jiang et al. [101] indicated that the increase in pore connectivity could also promote the improvement of movable oil saturation (i.e., the ratio of movable oil volume to pore volume, calculated by

nuclear magnetic resonance). By and large, the development characteristics of shale pores exert an important role in controlling oil content, which is the key to whether shale oil can be enriched [57,58].

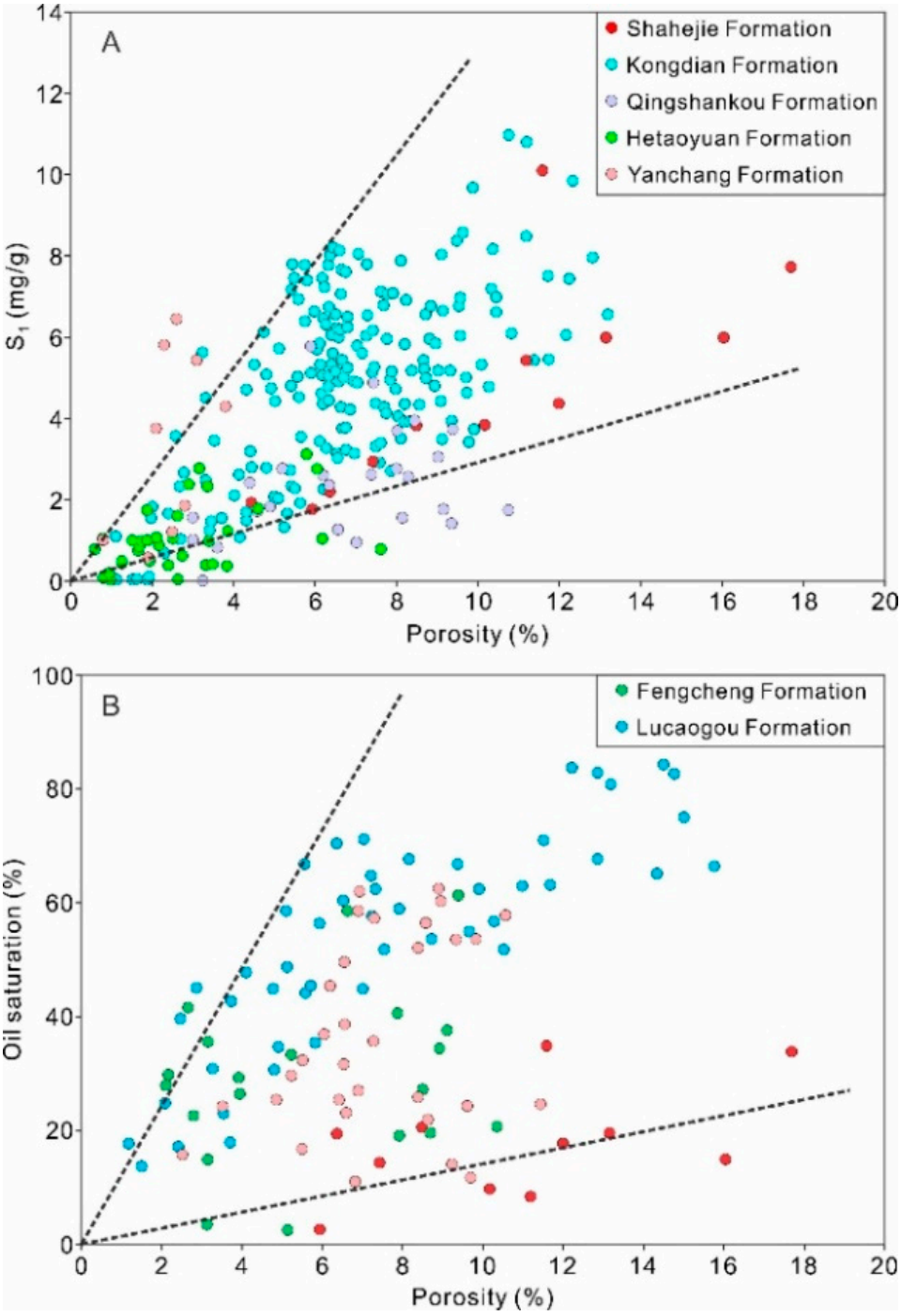

Figure 3. The relationship between porosity and S_1 (**A**) and oil saturation (**B**). Date from [46,79,98–100].

3.4. Restriction of Preservation Condition on Oiliness

The limited mobility of oil molecules compared to gas molecules suggests that preservation conditions for oil reservoirs are relatively less stringent [22]. However, this does not mean that the importance of preservation conditions can be ignored. The preservation conditions of the shale system mainly include the fracture development degree and scale and the sealing ability of the overlying or underlying tight reservoirs [75,102–104]. On the one hand, micro-fractures are important storage spaces for shale oil, and the increase in development provides conditions for the enrichment of shale oil [40,50]. Zhao et al. [59] found that when the overlying layer of shale is not destroyed, the greater the degree of micro-fractures, the higher the oil test yield. In the case of fault-related fracture development, on the other hand, the micro-fractures can act as a "bridge" to link microscopic pores and macro-fractures, leading to a large dispersion of oil molecules [105–107]. As a result, shale oil abundance in shale reservoirs is low and even without oil [22,108]. The exploration practice claimed that the distance between high-yield wells and faults in the Jiyang Depression is generally more than 100 m [75,103]. Quantitative calculations also show that the shale oil retention degree of the Lucaogou Formation in the Miquan area of the Junggar Basin is only 21.1% under strong tectonic action [109]. Collectively, a relatively stable tectonic environment is conducive to the preservation of retained oil in shales, forming high oil abundance [22,77,108].

4. Influence of Laminae on Shale Oil Content

4.1. Laminae and Quality of Source Rock

The source rock quality is closely related to organic matter content. Generally, with the increase in TOC content, the amount of generated hydrocarbons will also rise [42]. The predecessors generally used TOC of 2% as the boundary to determine the quality of terrestrial source rocks. Those with TOC content greater than 2% are classified as organic-rich shales, indicating that the source rock quality is good [29,30,108]. Previous works have noticed that the degree of development of lamina is highly correlated with TOC content [10,15,40]. In a laminated shale system, the rigid laminae and plastic laminae often appear alternately and superimposed vertically [10,110]. More importantly, plastic laminae are mainly composed of clay and organic matter [38,40]. On this premise, the more densely developed the lamina is, the more clay and organic matter layers are present, which in turn increases organic matter abundance. Our statistical results also suggest that the TOC content of laminated shales is superior, and more than 80% of the samples are organic-rich shales. The TOC of some samples even exceeded 12% (Figure 4). Compared to the laminated shale, however, the TOC value of massive shale is significantly lower. The peak value of TOC moves to <2%, indicating that the massive shale is dominated by organic-poor shale (Figure 4). A similar phenomenon has been widely reported in previous works [28,29,40,43,87,88]. Moreover, Zeng et al. [40] state that the type of lamina also controls organic matter enrichment, and the average TOC content of the fine lamina is higher than that of the wide lamina. Shi et al. [10] revealed that shale with high laminar continuity exhibits greater oil generation potential.

The hydrogen index expressed as HI = (S_2/TOC) × 100 (note: S_2 is the amount of hydrocarbons generated by pyrolysis between 300 °C and 650 °C, mg petroleum/g rock), is an important indicator to reveal the potential of kerogen in a rock to generate hydrocarbon [54]. The distribution characteristics of HI in different structural shales are similar to those of TOC, i.e., the values of HI show laminated shales > layered shales > massive shales (Figure 4). Xin et al. [28] also exhibited that most laminated shales have good to excellent hydrocarbon generation potential, while that of massive shales is dominated by poor to fair potential. These results demonstrated that laminar structure has a significant effect on hydrocarbon generation intensity [15,44,87].

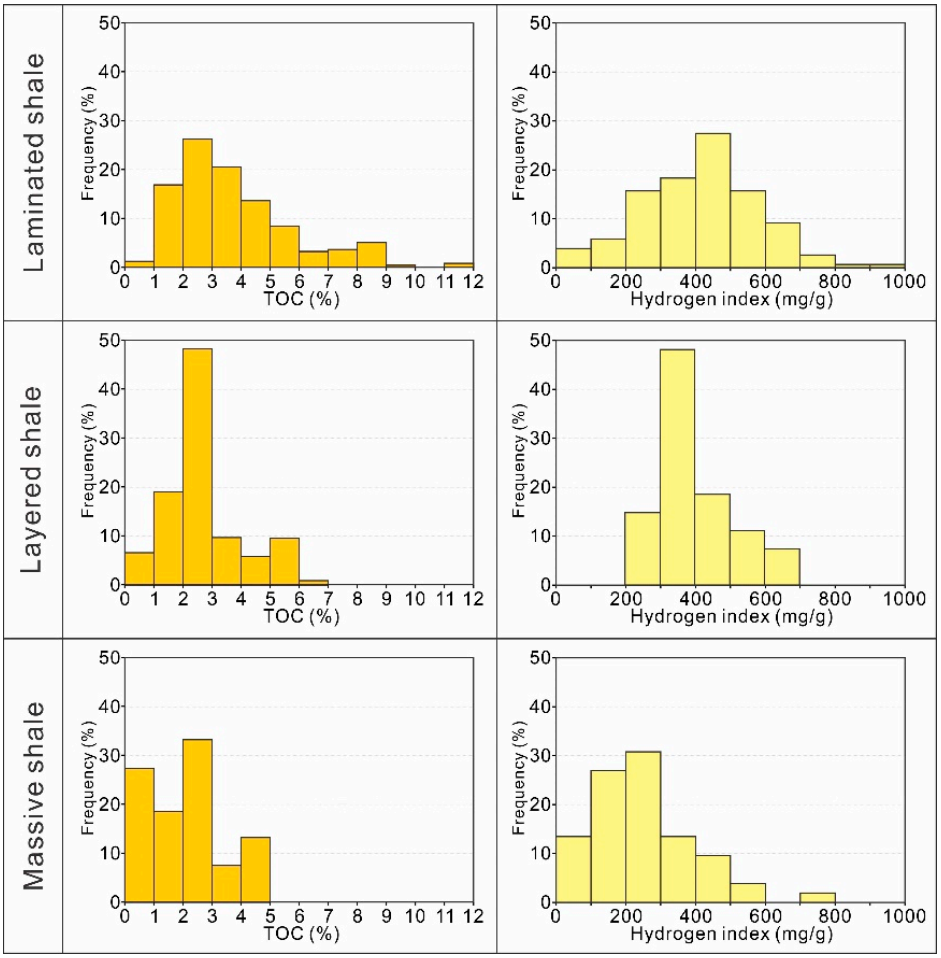

Figure 4. Distribution characteristics of TOC and hydrogen index for different types of shale. Date from [28,43,87–89,111].

4.2. Laminae and Storage Property

As mentioned above, the laminar structure is generally composed of alternating brittle laminae and plastic laminae in the vertical direction [11,110]. The interfaces between different laminae belong to weak surfaces, resulting in a significant fracture strength parallel to laminae smaller than that perpendicular to laminae [112–114]. During the diagenetic evolution process, the pore fluid pressure gradually increases and easily breaks through at these weak surfaces to form micro-fractures developed along the layers [112]. The reservoir property (e.g., porosity and permeability) of the shale reservoir is largely improved. The systematic comparison of reservoir characteristics in multiple sets of shales, e.g., Shahejie Formation shale, Kongdian Formation shale, and Lucaogou Formation shale, with different structures is conducted [44,76,111,115,116] (Figure 5). The wide porosity distribution and the high average value of lamellar shales indicate this type of shale has superior reservoir properties [29,75,76,87,111,117]. The well-developed micro-fractures also make lamellar shales possess a larger average pore size. This phenomenon is confirmed by the pore size distribution from the splicing of low-temperature nitrogen adsorption and mercury injection capillary pressure (MICP) data, as well as nuclear magnetic resonance (NMR) transverse relaxation time (T_2) spectra (Figure 5). Especially the MICP data conducted by Bao [111] and Zhang et al. [115] revealed that pores with a size above 100 nm are widely recognized in laminated shales but are not observed in massive shales. In addition, Zhao et al. [116] performed the nano-CT scans on laminated shales, layered shales, and massive shales in the Kongdian Formation of the Huanghu Depression. As presented in Figure 5, the results from nano-CT scanning indicate that the pores of the laminated shales are connected

by large throats and own great connectivity along the laminar direction. However, the pores of massive shales have no dominant direction in space and are mainly connected by small throats [116]. The pore connectivity of massive shales in three-dimensional space is limited (Figure 5). Furthermore, Shi et al. [10] found that pore structure is also related to laminar structure. Generally, the porosity of laminar shales with good continuity is higher than those of laminar shale with poor continuity [10].

To summarize from above discussion, the development of laminae improves the shale reservoir property, mainly including porosity, pore size, and pore connectivity. All these parameters provide an effective guarantee for shale oil enrichment [57,70,87,89,116].

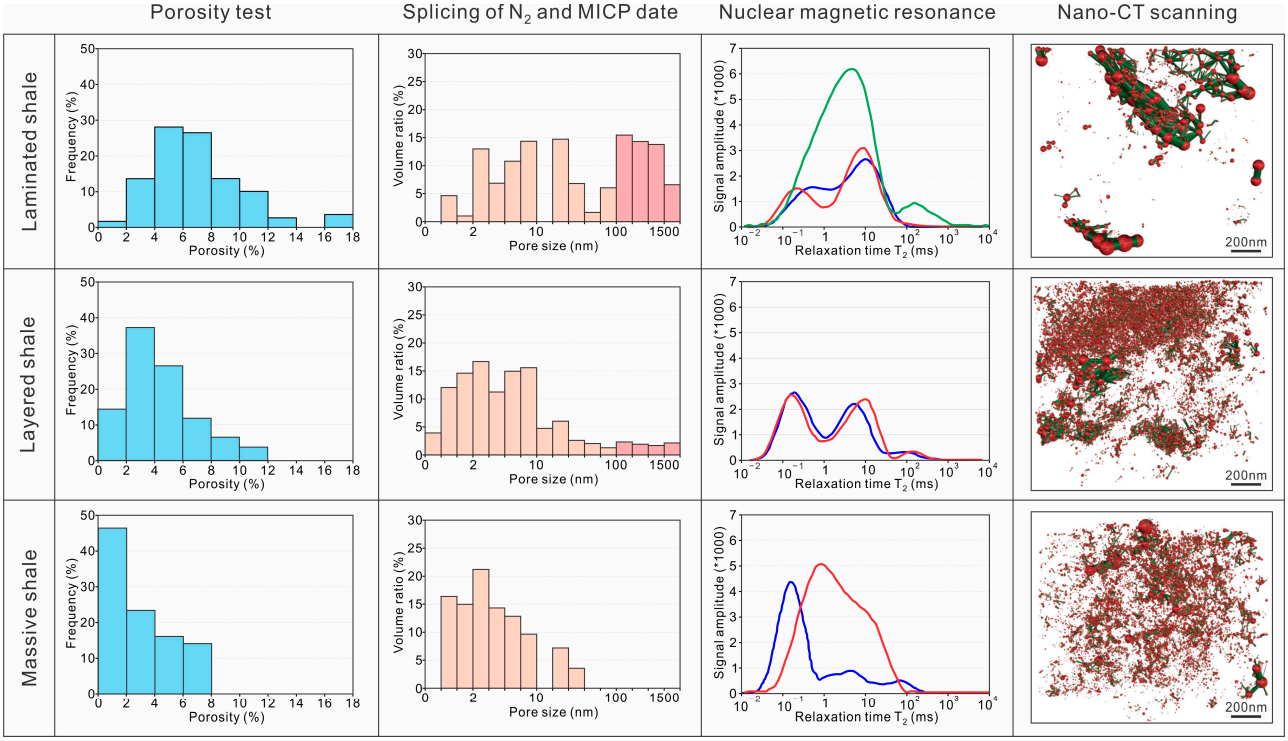

Figure 5. Distribution characteristics of porosity, pore size, NMR, and Nano-CT scanning for different types of shale. Date from [29,44,75,76,111,115,116].

4.3. Laminae and Expulsion Efficiency of Shale Oil

It is well known that micro-fractures are both an important storage space for hydrocarbons and a major channel for their transport and seepage [60,61,118]. Therefore, the development of lamina can have an impact on permeability while providing shale reservoir physical properties [29,76]. The experimental results of the permeability test show that the permeability of Qianjiang Formation shale in the Jianghan Basin is significantly different for samples with different laminae development degrees [22]. The horizontal permeability of shale with interlayer micro-fractures can reach 1000 times that of shale without interlayer micro-fractures [22]. Differences of tens to hundreds of times about this value have also been reported in the Shahejie Formation shale in the Jiyang depression [76]. Therefore, the laminar structure will control the hydrocarbon expulsion efficiency in shale reservoirs, which in turn affects the degree of hydrocarbon enrichment [119–121]. Simulation experiments of hydrocarbon generation and expulsion reveal that when the Ro is larger than 0.9%, the laminated shale has a hydrocarbon expulsion efficiency of greater than 45%. The layered shale has a lower hydrocarbon expulsion efficiency of less than 20% in general [61,117]. Moreover, Wang et al. [29] also suggested that the order of the oil-discharge ratio is laminated shales > layered shales > massive shales (Figure 6). It is important to note that petroleum extracts usually consist of saturated hydrocarbons, aromatics, resins, and asphaltenes [9,122]. Overall, a preferential release of saturates over aromatics and

over polar compounds is illustrated [16,26,61,123]. Therefore, the laminated shales with great oil-discharge efficiency would also promote oil component physical fractionation and improve oil quality, which has an important impact on the later production of shale oil [14,26,123].

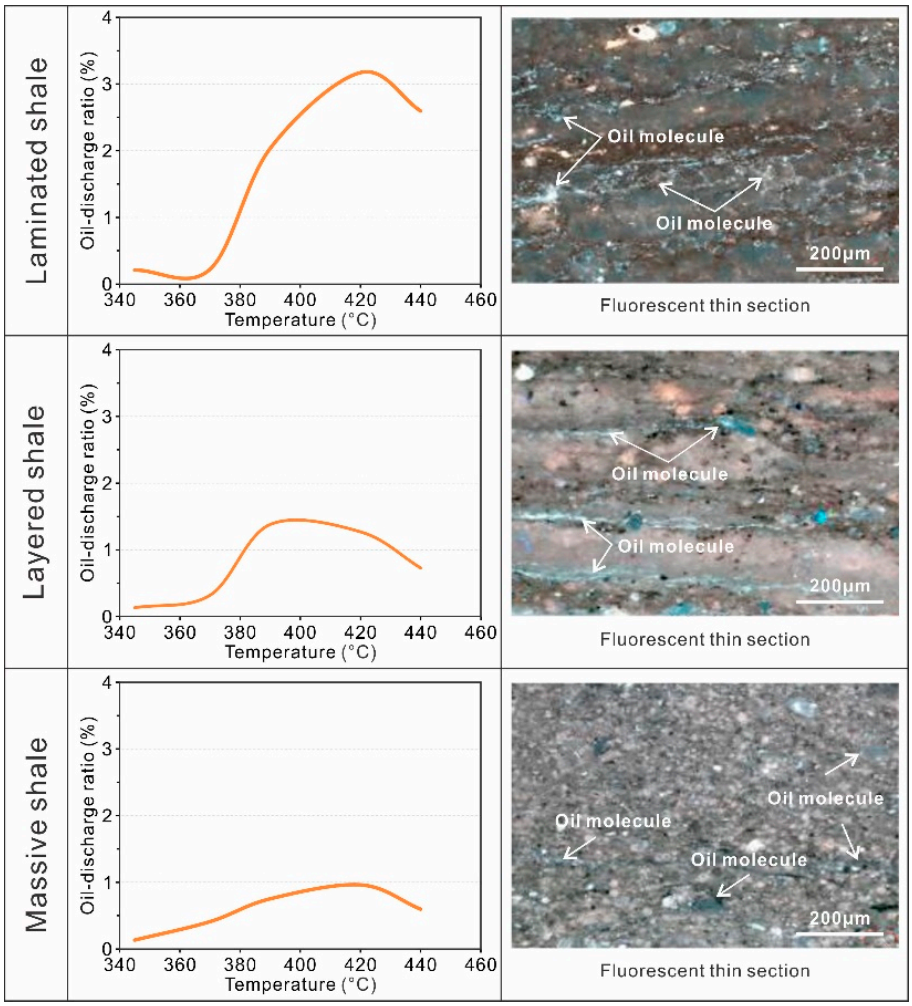

Figure 6. Oil-discharge ratio and hydrocarbon retention characteristics for different types of shale. Modified after [29,121].

Note that shales containing laminae, as mentioned above, exhibit a superior hydrocarbon generation ability (Figure 4). After the considerable amount of oil generation and meeting its storage requirements, the excess oil will be discharged to the adjacent layer [46,57]. In such cases, even if the oil expulsion efficiency of the laminated shale is high, the strong hydrocarbon generation capacity and superior storage space can still ensure that a large amount of oil molecules are retained in the shale system [29,119–121]. With the results, laminated shale exhibits intense blue fluorescence on thin sections, with linear distribution or local concentration of fluorescence along the lamination plane. However, the fluorescence intensity of massive shale is weak and scattered (Figure 6). Collectively, the oil-bearing of laminated shale is great, and the oil saturation and S_1 owned higher values. Additionally, the oil saturation index (OSI = S1 × 100/TOC) is considerable [75,87,111,124] (Figure 7). Plenty of researchers have also confirmed that laminae in shale can greatly influence the occurrence and amount of shale oil [10,15,70,125].

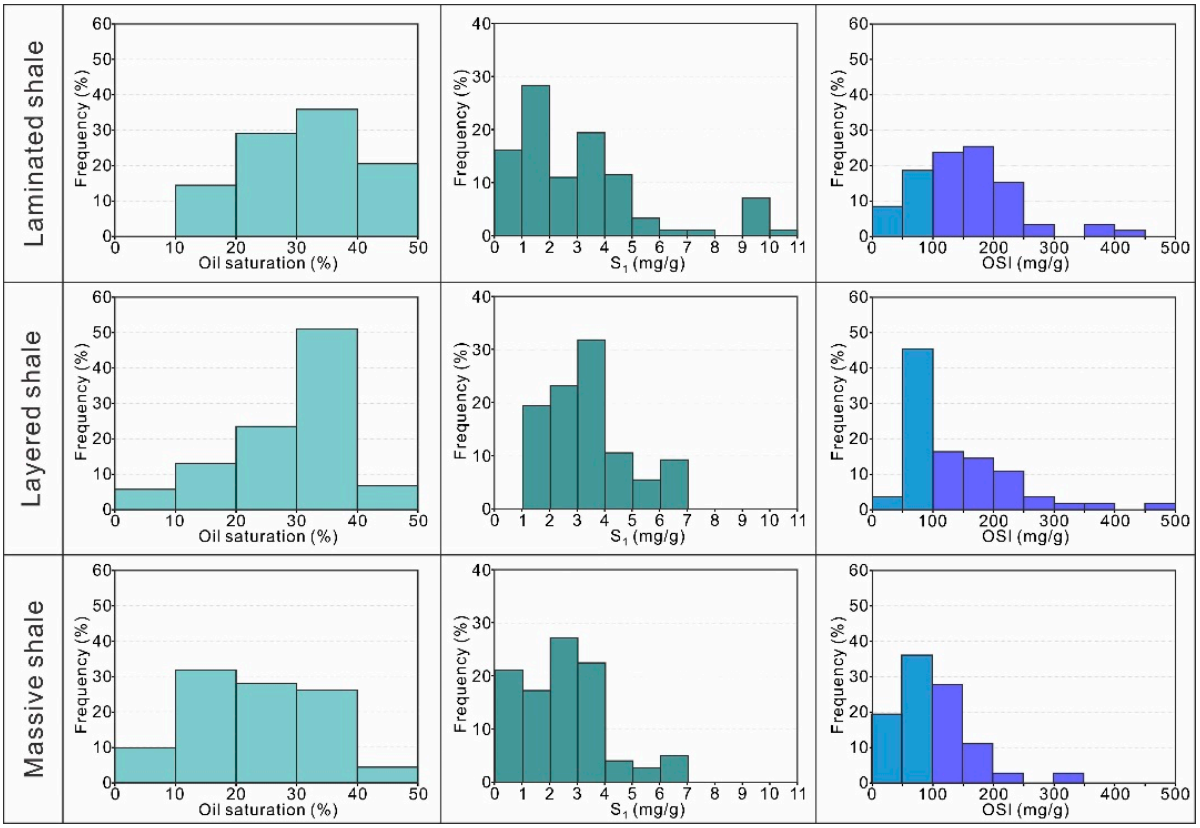

Figure 7. Distribution characteristics of oil saturation, S_1, and oil saturation index (OSI) for different types of shale. Date from [28,75,76,87,111,124].

5. Conclusions

(1) Mineral composition, thickness, continuity, geometry, color, and grain size are critical parameters for classifying shale lamination. However, the classification and terminology of shale laminae with different delineation schemes are often mutually inclusive. Therefore, a unified laminar capture scheme that can take into account various geological attributes needs to be proposed urgently.

(2) The oil-bearing property of shale reservoirs is influenced by a variety of factors. The type of organic matter, abundance, maturity, mineral composition, pore structure, and preservation conditions synergistically control the enrichment degree of petroleum molecules in the shale system. Generally, a shale system with aliphatic-rich organic matter, high TOC content, moderate Ro, excellent storage space, and great preservation condition generally has a superior shale oil content.

(3) As the degree of shale laminae development improves its hydrocarbon source rock quality and pore structure parameters (e.g., porosity and pore size) increase accordingly. However, the development of micro-fractures associated with laminae will also promote the transport and discharge of hydrocarbons. Overall, the strong hydrocarbon generation capacity and superior storage space make the lamellar shale still have considerable retention of petroleum even with high oil expulsion efficiency.

(4) The large pore size and good pore connectivity of laminated shale effectively improve the mobility of petroleum molecules, which is conducive to the high production of shale oil in the subsequent fracturing period. Combined with oil-bearing characteristics, thus, laminated shales are generally identified as sweet spot lithofacies for shale oil development in China. By doing so, the identification and prediction of laminae in the geological profile will be the focus of future work.

Author Contributions: Q.G.: conceptualization, methodology, software, formal analysis, investigation, resources, writing—original draft preparation, visualization; S.X.: validation, resources, data curation, writing—review and editing, supervision, project administration, funding acquisition. All authors have read and agreed to the published version of the manuscript.

Funding: This research was supported by the Shandong Provincial Key Research and Development Program (2020ZLYS08), the National Natural Science Foundation of China (42122017, 41821002), the independent innovation research program of China University of Petroleum (East China) (21CX06001A), and the Open Fund of Key Laboratory of Tectonics and Petroleum Resources (China University of Geosciences), Ministry of Education, China (TPR-2022-19). The project was supported by the Fundamental Research Funds for National Universities, China University of Geosciences (Wuhan).

Data Availability Statement: The data presented in this study is available on request from the corresponding author.

Conflicts of Interest: The authors declare that they have no conflict of interest.

References

1. Katz, B.; Lin, F. Lacustrine basin unconventional resource plays: Key differences. *Mar. Pet. Geol.* **2014**, *56*, 255–265. [CrossRef]
2. Jin, Z.; Liang, X.; Bai, Z. Exploration breakthrough and its significance of Gulong lacustrine shale oil in the Songliao Basin, Northeastern China. *Energy Geosci.* **2022**, *3*, 120–125. [CrossRef]
3. Li, Y.; Zhao, Q.; Lv, Q.; Xue, Z.; Cao, X.; Liu, Z. Evaluation technology and practice of continental shale oil development in China. *Pet. Explor. Dev.* **2022**, *49*, 1098–1109. [CrossRef]
4. Xu, S.; Gou, Q. The importance of laminae for China lacustrine shale oil enrichment: A review. *Energies* **2023**, *16*, 1661. [CrossRef]
5. U.S. Energy Information Administration (EIA). In *How Much Shale (Tight) Oil Is Produced in the United States?* US Department of Energy: Washington, DC, USA, 2020. Available online: https://www.eia.gov/tools/faqs/faq.php?id=847&t=6#:$\sim$:text=How%20much%20shale%20(tight)%20oil,resources%20in%20the%20United%20States (accessed on 4 October 2022).
6. U.S. Energy Information Administration (EIA). *International Energy Outlook 2019 with Projections to 2050*; US Energy Information Administration: Washington, DC, USA, 2019. Available online: https://www.eia.gov/outlooks/ieo/pdf/ieo2019.pdf (accessed on 2 February 2021).
7. Boak, J.; Kleinberg, R. Shale gas, tight oil, shale oil and hydraulic fracturing. In *Future Energy*; Elsevier: Amsterdam, The Netherlands, 2020; pp. 67–95. [CrossRef]
8. Sun, L.; Feng, Z.; Jiang, H.; Jiang, T. Responsibilities of petroleum prospectors: Discussions on dual logic and development trend of hydrocarbon exploration. *Pet. Explor. Dev.* **2021**, *48*, 999–1006. [CrossRef]
9. Zhao, X.; Zhou, L.; Pu, X.; Han, W.; Shi, Z.; Jing, F.; Xu, J.; Liu, X.; Guan, Q.; Chen, C.; et al. Theories, technologies and practices of lacustrine shale oil exploration and development: A case study of Paleogene Kongdian Formation in Cangdong sag, Bohai Bay Basin, China. *Pet. Explor. Dev.* **2022**, *49*, 707–718. [CrossRef]
10. Shi, J.; Jin, Z.; Liu, Q.; Zhang, T.; Fan, T.; Gao, Z. Laminar characteristics of lacustrine organic-rich shales and their significance for shale reservoir formation: A case study of the Paleogene shales in the Dongying Sag, Bohai Bay Basin, China. *J. Asian Earth Sci.* **2022**, *223*, 104976. [CrossRef]
11. Liu, H. Geological particularity and exploration practice of Paleogene shale oil in Jiyang depression: A case study of the upper submember of Member 4 to the lower submember of Member 3 of Shahejie Formation. *Acta Pet. Sin.* **2022**, *43*, 581.
12. Li, Q.; Xu, S.; Zhang, L.; Chen, F.; Wu, S.; Bai, N. Shale oil enrichment mechanism of the Paleogene Xingouzui Formation, Jianghan Basin, China. *Energies* **2022**, *15*, 4038. [CrossRef]
13. Yan, W.; Sun, F.; Sun, J.; Golsanami, N. Distribution model of fluid components and quantitative calculation of movable oil in inter-salt shale using 2D NMR. *Energies* **2021**, *14*, 2447. [CrossRef]
14. Zou, C.; Pan, S.; Horsfield, B.; Yang, Z.; Hao, S.; Liu, E.; Zhang, L. Oil retention and intrasource migration in the organic-rich lacustrine Chang 7 shale of the Upper Triassic Yanchang Formation, Ordos Basin, central China. *AAPG Bull.* **2019**, *103*, 2627–2663. [CrossRef]
15. Wu, S.; Zhu, R.; Luo, Z.; Yang, Z.; Jiang, X.; Lin, M.; Su, L. Laminar structure of typical continental shales and reservoir quality evaluation in central-western basins in China. *China Pet. Explor.* **2022**, *27*, 62–72. (In Chinese with English Abstract).
16. Guo, Q.; Yao, Y.; Hou, L.; Tang, S.; Pan, S.; Yang, F. Oil migration, retention, and differential accumulation in "sandwiched" lacustrine shale oil systems from the Chang 7 member of the Upper Triassic Yanchang Formation, Ordos Basin, China. *Int. J. Coal Geol.* **2022**, *261*, 104077. [CrossRef]
17. Pang, X.; Wang, G.; Kuang, L.; Li, H.; Zhao, Y.; Li, D.; Zhao, X.; Wu, S.; Feng, Z.; Lai, J. Insights into the pore structure and oil mobility in fine-grained sedimentary rocks: The Lucaogou Formation in Jimusar Sag, Junggar Basin, China. *Mar. Pet. Geol.* **2022**, *137*, 105492. [CrossRef]
18. Zhao, W.; Zhu, R.; Liu, W.; Bing, C.; Wang, K. Enrichment conditions and occurrence features of lacustrine mid-high matured shale oil in onshore China. *Earth Sci. Front.* **2023**, *30*, 116–127.

19. Zou, C.; Qiu, Z.; Zhang, J.; Li, Z.; Wei, H.; Liu, B.; Zhao, J.; Yang, T.; Zhu, S.; Tao, H.; et al. Unconventional petroleum sedimentology: A key to understanding unconventional hydrocarbon accumulation. *Engineering* **2022**, *18*, 62–78. [CrossRef]
20. Martin, R.; Baihly, J.; Malpani, R.; Atwood, W. Understanding Production from Eagle Ford-Austin chalk system. *Soc. Pet. Eng.* **2011**, *114117*, 1–28.
21. Jarvie, D.M. Components and processes affecting producibility and commerciality of shale resource systems. *Geol. Acta* **2014**, *12*, 307–325.
22. Jin, Z.; Zhu, R.; Liang, X.; Shen, Y. Several issues worthy of attention in current lacustrine shale oil exploration and development. *Pet. Explor. Dev.* **2021**, *48*, 1471–1484. [CrossRef]
23. Wang, E.; Feng, Y.; Guo, T.; Li, M. Oil content and resource quality evaluation methods for lacustrine shale: A review and a novel three-dimensional quality evaluation model. *Earth-Sci. Rev.* **2022**, *232*, 104134. [CrossRef]
24. Bohacs, K.M.; Carroll, A.R.; Neal, J.E.; Mankiewicz, P.J. Lake-basin type, source potential, and hydrocarbon character: An integrated sequence-stratigraphic-geochemical framework. Lake basins through space and time. *AAPG Stud. Geol.* **2000**, *46*, 3–34.
25. Zhao, K.; Du, X.; Lu, Y.; Xiong, S.; Wang, Y. Are light-dark coupled laminae in lacustrine shale seasonally controlled? A case study using astronomical tuning from 42.2 to 45.4 Ma in the Dongying Depression, Bohai Bay Basin, eastern China. Palaeogeography, Palaeoclimatolog. *Palaeoecology* **2019**, *528*, 35–49. [CrossRef]
26. Hu, S.; Bai, B.; Tao, S.; Bian, C.; Zhang, T.; Chen, Y.; Liang, X.; Wang, L.; Zhu, R.; Jia, J.; et al. Heterogeneous geological conditions and differential enrichment of medium and high maturity continental shale oil in China. *Pet. Explor. Dev.* **2022**, *49*, 257–271. [CrossRef]
27. Xu, Q.; Zhao, X.; Pu, X.; Han, W.; Shi, Z.; Tian, J.; Zhang, B.; Xin, B.; Guo, P. Characteristics and Control Mechanism of Lacustrine Shale Oil Reservoir in the Member 2 of Kongdian Formation in Cangdong Sag, Bohai Bay Basin, China. *Front. Earth Sci.* **2021**, *9*, 1144. [CrossRef]
28. Xin, B.; Zhao, X.; Hao, F.; Jin, F.; Pu, X.; Han, W.; Xu, Q.; Guo, P.; Tian, J. Laminae characteristics of lacustrine shales from the Paleogene Kongdian Formation in the Cangdong Sag, Bohai Bay Basin, China: Why do laminated shales have better reservoir physical properties? *Int. J. Coal Geol.* **2022**, *260*, 104056. [CrossRef]
29. Wang, Y.; Wang, X.; Song, G.; Liu, H.; Zhu, D.; Zhu, D.; Ding, J.; Yang, W.; Yin, Y.; Zhang, S.; et al. Genetic connection between mud shale lithofacies and shale oil enrichment in Jiyang Depression, Bohai Bay Basin. *Pet. Explor. Dev.* **2016**, *43*, 759–768. [CrossRef]
30. Song, M.; Liu, H.; Wang, Y.; Liu, Y. Enrichment rules and exploration practices of Paleogene shale oil in Jiyang Depression, Bohai Bay Basin, China. *Pet. Explor. Dev.* **2020**, *47*, 225–235. [CrossRef]
31. Kuroda, J.; Ohkouchi, N.; Ishii, T.; Tokuyama, H.; Taira, A. Lamina-scale analysis of sedimentary components in Cretaceous black shales by chemical compositional mapping: Implications for paleoenvironmental changes during the Oceanic Anoxic Events. *Geochim. Et Cosmochim. Acta* **2005**, *69*, 1479–1494. [CrossRef]
32. Li, L.; Huang, B.; Tan, Y.; Li, X.; Ranjith, P.G. Using micro-indentation to determine the elastic modulus of shale laminae and its implication: Cross-scale correlation of elastic modulus of mineral and rock. *Mar. Pet. Geol.* **2022**, *143*, 105740. [CrossRef]
33. Lazar, O.R.; Bohacs, K.M.; Macquaker, J.H.S.; Schieber, J.; Demko, T.M. Capturing key attributes of fine-grained sedimentary rocks in outcrops, cores, and thin sections: Nomenclature and description guidelines. *J. Sediment. Res.* **2015**, *85*, 230–246. [CrossRef]
34. Zolitschka, B.; Francus, P.; Ojala, A.E.K.; Schimmelmann, A. Varves in lake sediments—A review. *Quat. Sci. Rev.* **2015**, *117*, 1–41. [CrossRef]
35. Liu, H.; Wang, Y.; Yang, Y.; Zhang, S. Sedimentary environment and lithofacies of fine-grained hybrid in Dongying Sag: A case of fine-grained sedimentary system of the Es4. *Earth Sci.* **2020**, *45*, 3543–3555. (In Chinese with English Abstract).
36. Li, L.; Huang, B.; Li, Y.; Hu, R.; Li, X. Multi-scale modeling of shale laminas and fracture networks in the Yanchang formation, Southern Ordos Basin, China. *Eng. Geol.* **2018**, *243*, 231–240. [CrossRef]
37. Woo, J.; Lee, H.S.; Ozyer, C.; Rhee, C.W. Effect of lamination on shale reservoir properties: Case study of the Montney Formation, Canada. *Geofluids* **2021**, *2021*, 8853639. [CrossRef]
38. Hua, G.; Wu, S.; Qiu, Z.; Jing, Z.; Xu, J.; Guan, M. Lamination texture and its effect on reservoir properties: A case study of Longmaxi Shale, Sichuan Basin. *Acta Sedimentol. Sin.* **2021**, *32*, 1–22.
39. Pang, X.; Wang, G.; Kuang, L.; Kuang, L.; Lai, J.; Gao, Y.; Zhao, Y.; Li, H.; Wang, S.; Bao, M.; et al. Prediction of multiscale laminae structure and reservoir quality in fine-grained sedimentary rocks: The Permian Lucaogou Formation in Jimusar Sag, Junggar Basin. *Pet. Sci.* **2022**, *19*, 2549–2571. [CrossRef]
40. Zeng, X.; Cai, J.; Dong, Z.; Bian, L.; Li, Y. Relationship between mineral and organic matter in shales: The case of shahejie formation, Dongying Sag, China. *Minerals* **2018**, *8*, 222. [CrossRef]
41. Chen, Y.; Hu, Q.; Zhao, J.; Meng, M.; Yin, N.; Zhang, X.; Xu, G.; Liu, H. Lamina characteristics and their influence on reservoir property of lacustrine organic-rich shale in the Dongying Sag, Bohai Bay Basin. *Oil Gas Geol.* **2022**, *43*, 307–324. (In Chinese with English Abstract).
42. Zhao, X.; Pu, X.; Zhou, L.; Jin, F.; Shi, Z.; Han, W.; Jiang, W.; Zhang, W. Typical geological characteristics and exploration practices of lacustrine shale oil: A case study of the Kong-2 member strata of the Cangdong Sag in the Bohai Bay Basin. *Mar. Pet. Geol.* **2020**, *113*, 103999.

43. Zeng, X.; Cai, J.; Dong, Z.; Wang, X.; Hao, Y. Sedimentary characteristics and hydrocarbon generation potential of mudstone and shale: A case study of Middle Submember of Member 3 and Upper Submember of Member 4 in Shahejie Formation in Dongying sag. *Acta Pet. Sin.* **2017**, *38*, 31–43.
44. Sun, H. Exploration practice and cognitions of shale oil in Jiyang depression. *China Pet. Explor.* **2017**, *22*, 1–14.
45. Wang, M.; Chen, Y.; Song, G.; Steele-MacInnis, M.; Liu, Q.; Wang, X.; Zhang, X.; Zhao, Z.; Liu, W.; Zhang, H.; et al. Formation of bedding-parallel, fibrous calcite veins in laminated source rocks of the Eocene Dongying Depression: A growth model based on petrographic observations. *Int. J. Coal Geol.* **2018**, *200*, 18–35. [CrossRef]
46. Han, W.; Zhao, X.; Jin, M.; Pu, X.; Chen, X.; Mu, L.; Zhang, W.; Shi, Z.; Wang, H. Sweet spots evaluation and exploration of lacustrine shale oil of the 2nd member of Paleogene Kongdian Formation in Cangdong sag, Dagang Oilfield, China. *Pet. Explor. Dev.* **2021**, *48*, 1–10. [CrossRef]
47. Xi, K.; Li, K.; Cao, Y.; Lin, M.; Niu, X.; Zhu, R.; Wei, X.; You, Y.; Liang, X.; Feng, S. Laminae combination and shale oil enrichment patterns of Chang 73 sub-member organic-rich shales in the Triassic Yanchang Formation, Ordos Basin, NW China. *Pet. Explor. Dev.* **2020**, *47*, 1342–1353. [CrossRef]
48. Ingram, R.L. Terminology for the thickness of stratification and parting units in sedimentary rocks. *Geol. Soc. Am. Bull.* **1954**, *65*, 937–938. [CrossRef]
49. Dong, C.; Ma, C.; Lin, C.; Sun, X.; Yuan, M. A method of classification of shale set. *J. China Univ. Pet. (Ed. Nat. Sci.)* **2015**, *39*, 1–7. (In Chinese with English Abstract).
50. Li, M.; Wu, S.; Hu, S.; Zhu, R.; Meng, S.; Yang, J. Lamination Texture and Its Effects on Reservoir and Geochemical Properties of the Palaeogene Kongdian Formation in the Cangdong Sag, Bohai Bay Basin, China. *Minerals* **2021**, *11*, 1360. [CrossRef]
51. Yawar, Z.; Schieber, J. On the origin of silt laminae in laminated shales. *Sedimentary Geology* **2017**, *360*, 22–34. [CrossRef]
52. Bowker, K.A. Barnett shale gas production, Fort Worth Basin: Issues and discussion. *AAPG Bull.* **2007**, *91*, 523–533. [CrossRef]
53. Romero-Sarmiento, M.F.; Rouzaud, J.N.; Bernard, S.; Deldicque, D.; Thomas, M.; Littke, R. Evolution of Barnett Shale organic carbon structure and nanostructure with increasing maturation. *Org. Geochem.* **2014**, *71*, 7–16. [CrossRef]
54. Jarvie, D.M. Shale resource systems for oil and gas: Part 2—Shale-oil resource systems. In *Shale Reservoirs—Giant Resources for the 21st Century*; Breyer, J.A., Ed.; AAPG Memoir 97: Humble, TX, USA, 2012; pp. 89–119.
55. Spigolon, A.L.D.; Lewan, M.D.; de Barros Penteado, H.L.; Coutinho, L.F.C.; Mendonça Filho, J.G. Evaluation of the petroleum composition and quality with increasing thermal maturity as simulated by hydrous pyrolysis: A case study using a Brazilian source rock with Type I kerogen. *Org. Geochem.* **2015**, *83*, 27–53. [CrossRef]
56. Burnham, A.K. *Global Chemical Kinetics of Fossil Fuels: How to Model Maturation and Pyrolysis*; Springer: Cham, Switzerland, 2017; pp. 75–105.
57. Feng, Y.; Xiao, X.; Wang, E.; Sun, J.; Gao, P. Oil retention in shales: A review of the mechanism, controls and assessment. *Front. Earth Sci.* **2021**, *9*, 720839. [CrossRef]
58. Zhao, W.; Hu, S.; Hou, L.; Yang, T.; Li, X.; Guo, B.; Yang, Z. Types and resource potential of continental shale oil in China and its boundary with tight oil. *Pet. Explor. Dev.* **2020**, *47*, 1–11. [CrossRef]
59. Zhao, X.; Zhou, L.; Pu, X.; Jin, F.; Shi, Z.; Xiao, D.; Han, W.; Jiang, W.; Zhang, W.; Wang, H. Favorable formation conditions and enrichment characteristics of lacustrine facies shale oil in faulted lake basin: A case study of Member 2 of Kongdian Formation in Cangdong Sag, Bohai Bay Basin. *Acta Pet. Sin.* **2019**, *40*, 1013–1029. (In Chinese with English Abstract).
60. Katz, B.J.; Arango, I. Organic porosity: A geochemist's view of the current state of understanding. *Org. Geochem.* **2018**, *123*, 1–16. [CrossRef]
61. Du, J.; Hu, S.; Pang, Z.; Lin, J.; Hou, L.; Zhu, R. The types, potentials and prospects of continental shale oil in China. *China Pet. Explor.* **2019**, *24*, 560–568.
62. Cardott, B.J. Thermal maturity of Woodford Shale gas and oil plays, Oklahoma, USA. *Int. J. Coal Geol.* **2012**, *103*, 109–119. [CrossRef]
63. Yang, Z.; Zou, C. "Exploring petroleum inside source kitchen": Connotation and prospects of source rock oil and gas. *Pet. Explor. Dev.* **2019**, *46*, 181–193. [CrossRef]
64. Vandenbroucke, M. Kerogen: From Types to Models of Chemical Structure. *Oil Gas Sci. Technol.* **2006**, *58*, 243–269. [CrossRef]
65. Vandenbroucke, M.; Largeau, C. Kerogen origin, evolution and structure. *Org. Geochem.* **2007**, *38*, 719–833. [CrossRef]
66. Li, M.; Ma, X.; Jiang, Q.; Li, Z.; Pang, X.; Zhang, C. Enlightenment from formation conditions and enrichment characteristics of marine shale oil in North America. *Editor. Dep. Pet. Geol. Recovery Effic.* **2019**, *26*, 13–28. (In Chinese with English Abstract).
67. Zhao, W.; Zhang, B.; Wang, X.; Wu, S.; Zhang, S.; Liu, W.; Wang, K.; Zhao, X. Differences in source kitchens for lacustrine in-source and out-of-source hydrocarbon accumulations. *Pet. Explor. Dev.* **2021**, *48*, 541–554. [CrossRef]
68. Sun, J.; Xiao, X.; Cheng, P.; Wang, M.; Tian, H. The relationship between oil generation, expulsion and retention of lacustrine shales: Based on pyrolysis simulation experiments. *J. Pet. Sci. Eng.* **2021**, *196*, 107625. [CrossRef]
69. Li, J.; Wang, W.; Cao, Q.; Shi, Y.; Yan, X.; Tian, S. Impact of hydrocarbon expulsion efficiency of continental shale upon shale oil accumulations in eastern China. *Mar. Pet. Geol.* **2015**, *59*, 467–479.
70. Guan, M.; Liu, X.; Jin, Z.; Lai, J.; Liu, J.; Sun, B.; Liu, T.; Hua, Z.; Xu, W.; Shu, H.; et al. Quantitative characterization of various oil contents and spatial distribution in lacustrine shales: Insight from petroleum compositional characteristics derived from programed pyrolysis. *Mar. Pet. Geol.* **2022**, *138*, 105522. [CrossRef]

71. Pokrovsky, O.S.; Schott, J. Kinetics and mechanisms of dolomite dissolution in neutral to alkaline solutions revisited. *Am. J. Sci.* **2001**, *301*, 597–626. [CrossRef]
72. Seewald, J.S. Organic-inorganic interactions in petroleum-producing sedimentary basins. *Nature* **2003**, *426*, 327–333. [CrossRef]
73. Wang, Y.; Cao, Y.; Ma, B.; Liu, H.; Gao, Y.; Chen, L. Mechanism of diagenetic trap formation in nearshore subaqueous fans on steep rift lacustrine basin slopes-A case study from the Shahejie Formation on the north slope of the Minfeng Subsag, Bohai Basin, China. *Pet. Sci.* **2014**, *11*, 481–494. [CrossRef]
74. Liang, C.; Cao, Y.; Liu, K.; Jiang, Z.; Wu, J.; Hao, F. Diagenetic variation at the lamina scale in lacustrine organic-rich shales: Implications for hydrocarbon migration and accumulation. *Geochim. Et Cosmochim. Acta* **2018**, *229*, 112–128. [CrossRef]
75. Ning, F. The main control factors of shale oil enrichment in Jiyang depression. *Acta Pet. Sin.* **2015**, *36*, 905–914. (In Chinese with English Abstract).
76. Ning, F.; Wang, X.; Hao, X.; Yang, W.; Yin, Y.; Ding, J.; Zhu, D.; Zhu, D.; Zhu, J. Occurrence mechanism of shale oil with different lithofacies in Jiyang Depression. *Acta Pet. Sin.* **2017**, *38*, 185–195. (In Chinese with English Abstract).
77. Zhao, W.; Zhu, R.; Hu, S.; Hou, L.; Wu, S. Accumulation contribution differences between lacustrine organic-rich shales and mudstones and their significance in shale oil evaluation. *Pet. Explor. Dev.* **2020**, *47*, 1160–1171. [CrossRef]
78. Lu, S.; Huang, W.; Chen, F.; Li, J.; Wang, M.; Xue, H.; Wang, W.; Cai, X. Classification and evaluation criteria of shale oil and gas resources: Discussion and application. *Pet. Explor. Dev.* **2012**, *39*, 268–276. [CrossRef]
79. Feng, G.; Li, J.; Liu, J.; Zhang, X.; Yu, Z.; Tan, J. Discussion on the enrichment and mobility of continental shale oil in Biyang Depression. *Oil Gas Geol.* **2019**, *40*, 1236–1245. (In Chinese with English Abstract).
80. Li, T.; Liu, B.; Zhou, X.; Yu, H.; Xie, X.; Xie, Z.; Wang, X.; Rao, H. Classification and evaluation of shale oil enrichment: Lower third member of Shahejie Formation, Zhanhua Sag, Eastern China. *Mar. Pet. Geol.* **2022**, *143*, 105824. [CrossRef]
81. Yusupova, T.N.; Romanova, U.G.; Gorbachuk, V.V.; Muslimov, R.K.; Romanov, G.V. Estimation of the adsorption capacity of oil-bearing rocks: A method and its prospects. *J. Pet. Sci. Eng.* **2002**, *33*, 173–183. [CrossRef]
82. Dudášová, D.; Sébastien, S.; Hemmingsen, P.V.; Sjöblom, J. Study of asphaltenes adsorption onto different minerals and clays: Part 1. Experimental adsorption with UV depletion detection. *Colloids Surf. A Physicochem. Eng. Asp.* **2008**, *317*, 1–9. [CrossRef]
83. Li, Z.; Zou, Y.; Xu, X.; Sun, J.; Li, M.; Peng, P. Adsorption of mudstone source rock for shale oil–Experiments, model and a case study. *Org. Geochem.* **2016**, *92*, 55–62. [CrossRef]
84. Tian, S.; Erastova, V.; Lu, S.; Greenwell, H.C.; Underwood, T.R.; Xue, H.; Zeng, F.; Chen, G.; Wu, C.; Zhao, R. Understanding model crude oil component interactions on kaolinite silicate and aluminol surfaces: Toward improved understanding of shale oil recovery. *Energy Fuels* **2018**, *32*, 1155–1165. [CrossRef]
85. Ribeiro, R.C.; Correia, J.C.G.; Seidl, P.R. The influence of different minerals on the mechanical resistance of asphalt mixtures. *J. Pet. Sci. Eng.* **2009**, *65*, 171–174. [CrossRef]
86. Mohammadi, M.; Sedighi, M. Modification of Langmuir isotherm for the adsorption of asphaltene or resin onto calcite mineral surface: Comparison of linear and non-linear methods. *Prot. Met. Phys. Chem. Surf.* **2013**, *49*, 460–470. [CrossRef]
87. Wang, M.; Ma, R.; Li, J.; Lu, S.; Li, C.; Guo, Z.; Li, Z. Occurrence mechanism of lacustrine shale oil in the Paleogene Shahejie Formation of Jiyang depression, Bohai Bay Basin, China. *Pet. Explor. Dev.* **2019**, *46*, 833–846. [CrossRef]
88. Chen, F.; Zhao, H.; Lu, S.; Ding, X.; Ju, Y. The effects of composition, laminar structure and burial depth on connected pore characteristics in a shale oil reservoir, the Raoyang Sag of the Bohai Bay Basin, China. *Mar. Pet. Geol.* **2019**, *101*, 290–302. [CrossRef]
89. Ning, C.; Ma, Z.; Jiang, Z.; Su, S.; Li, T.; Zheng, L.; Wang, G.; Li, F. Effect of shale reservoir characteristics on shale oil movability in the lower third member of the Shahejie Formation, Zhanhua Sag. *Acta Geol. Sin.-Engl. Ed.* **2020**, *94*, 352–363. [CrossRef]
90. Feng, Z.; Liu, B.; Sao, H.; Wang, C.; Hong, S.; Wang, J.; Pan, H.; Wang, Y.; Zhang, A.; Tian, S.; et al. The diagenesis evolution and accumulating performance of the mud shale in Qingshankou Formation in Gulong area, Songliao Basin. *Pet. Geol. Oilfield Dev. Daqing* **2020**, *39*, 72–85. (In Chinese with English Abstract).
91. Cheng, P.; Xiao, X.; Fan, Q.; Gao, P. Oil Retention and Its Main Controlling Factors in Lacustrine Shales from the Dongying Sag, Bohai Bay Basin, Eastern China. *Energies* **2022**, *15*, 4270. [CrossRef]
92. Xu, Y.; Lun, Z.; Pan, Z.; Wang, H.; Zhou, X.; Zhao, C.; Zhang, D. Occurrence space and state of shale oil: A review. *J. Pet. Sci. Eng.* **2022**, *211*, 110183. [CrossRef]
93. Lu, S.; Xue, H.; Wang, M.; Xiao, D.; Huang, W.; Li, J.; Xie, L.; Tain, S.; Wang, S.; Li, J.; et al. Several key issues and research trends in evaluation of shale oil. *Acta Pet. Sin.* **2016**, *37*, 1309–1322.
94. Dang, W.; Nie, H.; Zhang, J.; Tang, X.; Jiang, S.; Wei, X.; Liu, Y.; Wang, F.; Li, P.; Chen, Z. Pore-scale mechanisms and characterization of light oil storage in shale nanopores: New method and insights. *Geosci. Front.* **2022**, *13*, 101424. [CrossRef]
95. Wang, S.; Feng, Q.; Javadpour, F.; Xia, T.; Li, Z. Oil adsorption in shale nanopores and its effect on recoverable oil-in-place. *Int. J. Coal Geol.* **2015**, *147*, 9–24. [CrossRef]
96. Zhang, S. Molecular dynamics simulation of shale oil occurrence in Dongying Depression. *Editor. Dep. Pet. Geol. Recovery Effic.* **2021**, *28*, 74–80. (In Chinese with English Abstract).
97. Chen, G.; Lu, S.; Zhang, J.; Pervukhina, M.; Liu, K.; Wang, M.; Han, T.; Tian, S.; Li, J.; Zhang, Y.; et al. A method for determining oil-bearing pore size distribution in shales: A case study from the Damintun Sag, China. *J. Pet. Sci. Eng.* **2018**, *166*, 673–678. [CrossRef]

98. Wang, B.; Liu, B.; Sun, G.; Bai, L.; Chi, Y.; Liu, Q.; Liu, M. Evaluation of the Shale Oil Reservoir and the Oil Enrichment Model for the First Member of the Lucaogou Formation, Western Jimusaer Depression, Junggar Basin, NW China. *ACS Omega* **2021**, *6*, 12081–12098. [CrossRef] [PubMed]
99. Li, P.; Jia, C.; Jin, Z.; Liu, Q.; Zheng, M.; Huang, Z. The characteristics of movable fluid in the Triassic lacustrine tight oil reservoir: A case study of the Chang 7 member of Xin'anbian Block, Ordos Basin, China. *Mar. Pet. Geol.* **2019**, *102*, 126–137. [CrossRef]
100. Xu, L.; Chang, Q.; Feng, L.; Zhang, N.; Liu, H. The reservoir characteristics and control factors of shale oil in Permian Fengcheng Formation of Mahu Sag, Junggar Basin. *China Pet. Explor.* **2019**, *24*, 649–660.
101. Jiang, Z.; Li, T.; Gong, H.; Jiang, T.; Chang, J.; Ning, C.; Su, S.; Chen, W. Characteristics of low-mature shale reservoirs in Zhanhua Sag and their influence on the mobility of shale oil. *Acta Pet. Sin.* **2020**, *41*, 1587–1600. (In Chinese with English Abstract).
102. Gou, Q.; Xu, S.; Hao, F.; Yang, F.; Shu, Z.; Liu, R. The effect of tectonic deformation and preservation condition on the shale pore structure using adsorption-based textural quantification and 3D image observation. *Energy* **2021**, *219*, 119579. [CrossRef]
103. Wang, Y.; Song, G.; Liu, H.; Jiang, X.; Hao, X.; Ning, F.; Zhu, D.; Lin, L. Main control factors of enrichment characteristics of shale oil in Jiyang depression. *Editor. Dep. Pet. Geol. Recovery Effic.* **2015**, *22*, 20–25. (In Chinese with English Abstract).
104. Gou, Q.; Xu, S.; Hao, F.; Lu, Y.; Shu, Z.; Lu, Y.; Wang, Z.; Wang, Y. Evaluation of the exploration prospect and risk of marine gas shale, southern China: A case study of Wufeng-Longmaxi shales in the Jiaoshiba area and Niutitang shales in the Cen'gong area. *GSA Bull.* **2022**, *134*, 1585–1602. [CrossRef]
105. Zhang, Z.; Xu, S.; Gou, Q.; Li, Q. Reservoir characteristics and resource potential of marine shale in South China: A review. *Energies* **2022**, *15*, 8696. [CrossRef]
106. Xu, S.; Gou, Q.; Hao, F.; Zhang, B.; Shu, Z.; Lu, Y.; Wang, Y. Shale pore structure characteristics of the high and low productivity wells, Jiaoshiba shale gas field, Sichuan Basin, China: Dominated by lithofacies or preservation condition? *Mar. Pet. Geol.* **2020**, *114*, 104211. [CrossRef]
107. Gou, Q.; Xu, S.; Hao, F.; Shu, Z.; Zhang, Z. Making sense of micro-fractures to the Longmaxi shale reservoir quality in the Jiaoshiba area, Sichuan Basin, China: Implications for the accumulation of shale gas. *J. Nat. Gas Sci. Eng.* **2021**, *94*, 104107. [CrossRef]
108. Liu, B.; Sun, J.; Zhang, Y.; He, J.; Fu, X.; Yang, L.; Xing, J.; Zhao, X. Reservoir space and enrichment model of shale oil in the first member of Cretaceous Qingshankou Formation in the Changling sag, southern Songliao Basin, NE China. *Pet. Explor. Dev.* **2021**, *48*, 608–624. [CrossRef]
109. Lin, H.; Song, M.; Wang, S.; Zhang, K. Shale oil resource evaluation in complex structural belt of superimposed basin: A case study of middle Permian Lucaogou Formation in Bogda area, southeast margin of Junggar Basin. *Editor. Dep. Pet. Geol. Recovery Effic.* **2020**, *27*, 7–17. (In Chinese with English Abstract).
110. Ma, C.; Dong, C.; Lin, C.; Elsworth, D.; Luan, G.; Sun, X.; Liu, X. Influencing factors and fracability of lacustrine shale oil reservoirs. *Mar. Pet. Geol.* **2019**, *110*, 463–471. [CrossRef]
111. Bao, Y. Effective reservoir spaces of Paleogene shale oil in the Dongying Depression, Bohai Bay Basin. *Pet. Geol. Expepiment* **2018**, *40*, 480–484. (In Chinese with English Abstract).
112. Mighani, S.; Sondergeld, C.H.; Rai, C.S. Observations of tensile fracturing of anisotropic rocks. *SPE J.* **2016**, *21*, 1289–1301. [CrossRef]
113. Xiong, Z.; Wang, G.; Cao, Y.; Liang, C.; Li, M.; Shi, X.; Zhang, B.; Li, J.; Fu, Y. Controlling effect of texture on fracability in lacustrine fine-grained sedimentary rocks. *Mar. Pet. Geol.* **2019**, *101*, 195–210. [CrossRef]
114. Ma, C.; Elsworth, D.; Dong, C.; Lin, C.; Luan, G.; Chen, B.; Liu, X.; Muhammad, J.M.; Muhammad, A.Z.; Shen, Z.; et al. Controls of hydrocarbon generation on the development of expulsion fractures in organic-rich shale: Based on the Paleogene Shahejie Formation in the Jiyang Depression, Bohai Bay Basin, East China. *Mar. Pet. Geol.* **2017**, *86*, 1406–1416. [CrossRef]
115. Zhang, L.; Bao, Y.; Xi, C. Pore Structure Characteristics and Pore Connectivity of Paleogene Shales in Dongying Depression. *Xinjiang Pet. Geol.* **2018**, *39*, 134–139. (In Chinese with English Abstract).
116. Zhao, X.; Pu, X.; Zhou, L.; Jin, F.; Han, G.; Shi, Z.; Han, W.; Ding, Y.; Zhang, W.; Wang, G.; et al. Enrichment theory, exploration technology and prospects of shale oil in lacustrine facies zone of deep basin: A case study of the Paleogene in Huanghua Depression, Bohai Bay Basin. *Acta Pet. Sin.* **2021**, *42*, 143–162.
117. Hu, S.; Zhao, W.; Hou, L.; Yang, Z.; Zhu, R.; Wu, S.; Bai, B.; Jin, X. Development potential and technical strategy of continental shale oil in China. *Pet. Explor. Dev.* **2020**, *47*, 877–887. [CrossRef]
118. Gou, Q.; Xu, S.; Hao, F.; Yang, F.; Zhang, B.; Shu, Z.; Zhang, A.; Wang, Y.; Lu, Y.; Cheng, X.; et al. Full-scale pores and micro-fractures characterization using FE-SEM, gas adsorption, nano-CT and micro-CT: A case study of the Silurian Longmaxi Formation shale in the Fuling area, Sichuan Basin, China. *Fuel* **2019**, *253*, 167–179. [CrossRef]
119. Zhang, S.; Zhang, L.; Zha, M. Research on simulation of hydrocarbon expulsion difference in lacustrine source rocks: A case study of Paleogene Es3 member in the Dongying Depression. *Pet. Geol. Recovery Effic.* **2009**, *16*, 32–35. (In Chinese with English Abstract).
120. Wang, Y.; Liu, H.; Song, G.; Jiang, X.; Zhu, D.; Zhu, D.; Yang, W.; Yin, Y.; Ding, J. Enrichment controls and models of shale oil in the Jiyang Depression, Bohai Bay Basin. *Geol. J. China Univ.* **2017**, *23*, 268–276. (In Chinese with English Abstract).
121. Jin, Q.; Zhang, H.; Cheng, F.; Xu, J. Stimulations on generation, expulsion and retention of liquid hydrocarbons in source rocks deposited in lacustrine basin and their significance in petroleum geology. *J. China Univ. Pet. (Ed. Nat. Sci.)* **2019**, *43*, 44–52. (In Chinese with English Abstract).

122. Ilyushin, Y.V.; Fetisov, V. Experience of virtual commissioning of a process control system for the production of high-paraffin oil. *Sci. Rep.* **2022**, *12*, 18415. [CrossRef]
123. Han, Y.; Horsfield, B.; LaReau, H.; Mahlstedt, N. Intraformational migration of petroleum: Insights into the development of sweet spot in the Cretaceous Niobrara shale-oil system, Denver Basin. *Mar. Pet. Geol.* **2019**, *107*, 301–309. [CrossRef]
124. Shao, X.; Pang, X.; Li, H.; Hu, T.; Xu, T.; Xu, Y.; Li, B. Pore network characteristics of lacustrine shales in the Dongpu Depression, Bohai Bay Basin, China, with implications for oil retention. *Mar. Pet. Geol.* **2018**, *96*, 457–473. [CrossRef]
125. Zhang, S.; Yan, J.; Hu, Q.; Wang, J.; Tian, T.; Chao, J.; Wang, M. Integrated NMR and FE-SEM methods for pore structure characterization of Shahejie shale from the Dongying Depression, Bohai Bay Basin. *Mar. Pet. Geol.* **2019**, *100*, 85–94. [CrossRef]